(2)

Technical Progress Report

The use of Air Force Cloud Cover Data to Evaluate and Improve Cloud Forecast & Parameterization in Mesoscale Meteorology Models

1 October 1991 - 30 September 1992

AF Office of Scientific Research # F49620-92-J0018

Prepared for:

Lt. Col. James G. Stobie, Program Manager
Air Force Office of Scientific Research
Building 410, Bolling AFB
Washington, D. C. 20332-6448

Prepared by:

Chris J. Walcek, Principal Investigator
Atmospheric Sciences Research Center
State University of New York at Albany
100 Fuller Rd.
Albany, NY 12205
(518) 442-3840

20 November 1992

REPORT DOCUMENTATION PAGE

25 Nov 92 ANNUAL/1 Oct 91 - 30 Sep 92

THE USE OF AIR FORCE CLOUD COVER DATA TO EVALUATE AND IMPROVE CLOUD FORECAST & PARAMETERIZATION IN MESOSCALE METEOROLOGY MODELS

PE 61102F
PR 2310
TA CS
F49621-92-J-0018

Chris J. Walcek

Atmospheric Sciences Research Center
State University of New York at Albany
100 Fuller Road
Albany NY 12205

AFOSR-TR-

AFOSR/NL
Building 410
Bolling AFB DC 20332-6448
Lt Col Stobie

Approved for public release;
distribution unlimited

This research program utilizes satellite and surfaced-derived cloud observations together with standard meteorological measurements to evaluate and improve our ability to accurately diagnose cloud coverage. Results of this research will be used to compliment existing or future parameterizations of cloud effects in global and regional-scale meteorology forecast models, since nearly all cloud parameterizations must specify a fractional area of cloud coverage when calculating radiative or dynamic cloud effects, and current parameterizations rely on rather crude cloud cover estimates.

			15 NUMBER OF PA
			16 PRICE CODE
(U)	(U)	(U)	UNLIMITED

1. Project Statement of Work

This research program utilizes satellite and surface-derived cloud observations together with standard meteorological measurements to evaluate and improve our ability to accurately diagnose cloud coverage. Results of this research will be used to compliment existing or future parameterizations of cloud effects in global and regional-scale meteorology forecast models, since nearly all cloud parameterizations must specify a fractional area of cloud coverage when calculating radiative or dynamic cloud effects, and current parameterizations rely on rather crude cloud cover estimates.

During the first phase of this research program, our goal is to evaluate and improve the methods for calculating cloud cover within a mesoscale meteorology model. To accomplish this, a mesoscale meteorology model will be quantitatively evaluated using the U. S. Air Force 3DNEPH and RTNEPH satellite-derived cloud fields. Hourly-averaged distributions of the model-derived cloud fields will be compared with observed clouds at the finest spatial and temporal resolution of the corresponding datasets. Algorithms currently used in global or mesoscale meteorological models to assess cloud coverage will be objectively evaluated. We will then carry out an innovative search for relationships between cloud coverage and numerous meteorological factors such as relative humidity, stability, wind shear, moisture convergence, precipitation rate and other parameters.

During the second phase of this research, the cloud cover data and improved parameterizations of cloud coverage developed during the first phase will be incorporated into a mesoscale meteorology model. Model forecasts which utilize the observed cloud coverage and depth should be improved relative to forecasts which crudely specify cloud properties.

2. Project Progress: 1 Oct. 1991 - 30 Sept. 1992

During the first year of this research program, we have compiled and reviewed a list of formulations used by various research groups to specify cloud cover. We find considerable variability between formulations used by various climate and meteorology models, and under some conditions, one formulation will produce a zero cloud amount, while an alternate formulation calculates 95% cloud cover under the same environmental conditions. All formulations hypothesize that cloud cover is predominantly determined by the average relative humidity, although some formulations allow local temperature lapse rates and vertical velocities to influence cloud amount. All formulations specify that cloud fraction is zero below a "threshold" relative humidity, and there are several estimates of this vertically-varying "threshold" based on physical arguments or "tuning" of free parameters to match global albedo estimates. We find that a majority of the formulations are based on limited observations, and evaluations of algorithm accuracy are based on longer-term compilations of cloud cover observations that cannot resolve the vertical distribution of cloud amount.

In order to explicitly evaluate the accuracy of these and future cloud cover algorithms, we have prepared an evaluation database of cloud cover and related meteorological observations during a springtime midlatitude cyclone. This growing dataset contains simultaneous observations of cloud cover fraction, moisture, wind speeds, temperatures at over 5000 $(320\ km)^2$ areas over the northeast U. S. at 15 tropospheric levels. Cloud cover is derived from the U. S. Air Force 3DNEPH satellite archive, and related meteorology is extracted from the NMC analysis. We have developed initial versions of a set of analysis programs designed to search for and quantify correlations between cloud cover and other meteorological factors. This cloud observational database is being used to assess the accuracy of existing cloud cover algorithms.

We find that most cloud cover algorithms tend to underpredict cloud coverage at any particular level in the troposphere, especially under dry conditions, when we find 10 - 20 % cloud cover at relative humidities as low as 20 - 30% within certain tropospheric layers averaged over $(320\ km)^2$ areas. We also find that cloud amount appears to increase with increasing humidity at all relative humidities, in stark contrast to existing formulations, which contain no cloud cover sensitivity to relative humidity at humidities below the 70 - 90 % "critical" humidities used by these models. We see no clear evidence that cloud cover vanishes at a "critical humidity". Based on these initial comparisons, we feel that current short-term meteorology models cannot adequately assess the *changes* in cloud cover that may results from small changes in relative humidity induced by larger-scale forcings. Additionally, a potentially important feedback between climate change and changes in cloud cover are probably not adequately simulated by current models of global warming.

We have discovered an apparent discrepancy between observed relative humidity in the upper troposphere under dry conditions, and calculations of relative humidity using the NCAR Mesoscale meteorology model, with the model calculating excessive relative humidity in the upper troposphere under unstable conditions. This is most likely attributable to an incorrect parameterization of moisture redistribution by the convective parameterization used by the model. Such an error would lead to an inaccurate cloud coverage calculation if it were present in a forecast model.

We have begun development of an improved convective-scale vertical mixing parameterization for use in our mesoscale meteorological model in order to alleviate the deficiency in the NCAR mesoscale meteorological model. At this point, the model is being tested as a stand-alone, single column model that is being tested with observations of tropical convection. This convective mixing algorithm will be based on a detraining cloud-plume description of buoyantly-driven cloud motions, and include a reasonably

sophisticated description of multi-stream cloud up- and down-drafts with somewhat more sophisticated microphysics than are currently incorporated into most cumulus parameterizations. This new cumulus parameterization will be used to assess the heating and moistening tendencies due to buoyantly-induced convection within hydrostatic models of the atmosphere that cannot explicitly compute these effects.

In addition to the time devoted by Dr. Walcek to this research effort, two post-doctoral research associates (Dr. Kesu Zhang and Dr. Hu Qi) and a graduate student are contributing to various technical aspects of this project. We have also purchased microcomputer and workstation-level computer software and hardware as needed by this project.

Dr. Walcek presented results from this research effort at two scientific meetings: the *11th International Conference on Clouds and Precipitation* held in Montreal, Canada, 17-21 August 1992; and the *WMO Cloud Microphysics and Applications to Global Climate Change Workshop* held in Toronto, Canada from 10-14 August 1992. We have also prepared a manuscript for journal publication summarizing the research results described above. Meeting abstracts citations are listed at the end of this progress report, and a copy of the reviewed manuscript (undergoing minor revisions) is provided with this report.

4. Budget Status:

As of 30 September 1992, 98% of the moneys budgeted for the first year have been expended approximately as initially budgeted. Moneys budgeted for computer expenses were used to purchase microcomputer and workstation hardware and software. Results of the initial analysis of cloud cover were presented at international meetings in Canada, and travel expenses associated with these meetings were included with the original budget. Costs associated with hiring an additional post-doctoral research associate (Dr. Hu Qi) to

assist in this research effort were also incurred during the year. Two candidates were considered for this position, and expenses associated with interviews were partially defrayed from this grant.

5. Plan for Next Year: 1 Oct. 1992 - 30 Sept. 1993

During the next funding year of this research effort, the cloud cover data and improved parameterizations of cloud coverage developed during the first phase will be incorporated into a mesoscale meteorology model. Model forecasts which utilize the observed cloud coverage and depth should be improved relative to forecasts which crudely specify cloud properties. During this period, we anticipate running improved versions of the MM4 meteorological model on USAF supercomputers. We plan to continue to expand our inter comparison dataset on which we analyze cloud cover and related meteorology. In addition to the springtime observation period, we will be simulating a summertime period in conjunction with RTNEPH data.

On 12 October 1992, Drs. Walcek and Zhang traveled to Phillips Laboratory near Boston to initiate a collaboration with Air Force scientists involved with similar research there. After presenting results to the cloud-analysis research group there, Dr. G. Modica familiarized us in the methods of running the mesoscale forecast model on USAF CRAY-2 computer. Considerable modifications to the run procedure are required to transfer the mesoscale meteorology model from the CRAY-YMP to the Phillips Laboratory Supercomputer Center. Fortunately, USAF scientists have experience with this transfer, and can thus save us considerable effort as our research progresses.

Conference presentations, abstracts, and journal manuscripts resulting from this research effort:

Walcek, C. J., 1992: Cloud cover and its relationship with relative humidity during a springtime midlatitude cyclone: some implications for climate models. Proceedings, *11th International Conference on Clouds and Precipitation*. Montreal, Canada, 17-21 August 1992. Elsevier Publishers, 1128-1131.

Walcek, C. J., 1992: Extrapolating cloud-scale microphysical, dynamic, and radiative processes to global and climatic scales: How accurately do we know the fractional area of cloud coverage?. Workshop proceedings of the *WMO Cloud Microphysics and Applications to Global Climate Change Workshop*. Toronto, Canada, 10-14 August 1992. In press.

Walcek, C. J., 1992: Cloud cover and its relationship with meteorological factors during a springtime midlatitude cyclone. *Monthly Weather Review*. manuscript submitted and under review, July 1992.

APPENDIX:

Manuscript submitted and reviewed by the journal
MONTHLY WEATHER REVIEW

This manuscript has been accepted for publication after minor revisions.
Following some minor revisions (in progress),
The article will be resubmitted during the month of November 1992.

Cloud cover and its relationship to other meteorological factors during a springtime midlatitude cyclone

CHRIS J. WALCEK

Atmospheric Sciences Research Center, State University of New York, Albany, New York

December 1992)

ABSTRACT

In this study, we compare vertical distributions of fractional cloud coverage within ~(320 km)^2 areas with co-located standard meteorological observations over the northeast U. S. during a springtime midlatitude cyclone. Cloud cover observations are derived from the U. S. Air Force 3DNEPH analysis of satellite imagery and surface-based reports. Standard meteorological parameters are interpolated from measurements using a hydrostatic mesoscale meteorology model.

Under conditions when no cumulus convection is possible, we find moderate to good positive correlations between cloud cover and relative humidity and large-scale vertical velocity, and evidence for weak negative correlations between cloud cover and wind shear and temperature lapse rate. We present contours of the mean fractional cloud coverage observed at various relative humidities and pressures, and suggest algorithms for estimating cloud coverage from humidity and/or vertical velocity. These comparisons suggest that cloud cover decreases exponentially as humidity falls below 100%. Relative to other layers in the troposphere, the middle troposphere (2.5 - 5 km above the surface) contains the highest cloud amounts at the lowest relative humidities, with mean cloud amounts of 30% near 50% humidity at 650 mb. At the same relative humidity, areas with large-scale upward motions contain higher cloud amounts than areas where subsidence is occurring.

Under convectively unstable conditions, we see evidence for increased cloud amounts relative to stable conditions at the same humidity in the upper troposphere at high humidities. In the lower troposphere, high humidity environments where convection is possible contain lower

cloud amounts relative to stable conditions at the same relative humidity, which may result from the subsidence of dry air into the lower troposphere under convectively unstable conditions. These findings must be interpreted with caution since we see evidence for excessive water vapor transport to the upper troposphere using the moisture convergence-based convective mixing algorithm within our dynamic meteorological interpolation algorithm. We find evidence for a bias in our area-averaged humidity estimates when interpolating from sparse, point radiosonde measurements under unstable conditions. More accurate methods of inferring cloud coverage from relative humidity will require more accurate methods of inferring moisture distributions over large areas, particularly within convectively unstable areas.

This analysis suggests that there is considerable uncertainty in measuring cloud cover and other meteorological factors averaged over large areas, suggesting that any formulations of cloud cover fraction are highly uncertain. Over a wide variety of meteorological environments associated with a springtime midlatitude cyclone, most cloud cover parameterizations used within meteorological, climate, and chemical models of the atmosphere calculate cloud amounts less than reported by the 3DNEPH observations, especially in the middle troposphere, where most algorithms specify zero cloud amounts at relative humidities below 50 - 80%. Thus, current large-scale climate simulations or atmospheric chemical modeling studies may significantly underestimate the effects of clouds. More importantly, current climate models probably cannot adequately estimate the potentially significant changes in cloud cover that can result from small changes in relative humidity.

1. Introduction

Microphysical and dynamical processes occurring within clouds can significantly influence numerous larger-scale dynamic, radiative, and chemical processes occurring in the troposphere (e.g. Arakawa and Schubert, 1974; Ramanathan et al., 1983; Walcek et al., 1990). Since clouds are frequently present, it is necessary for accurate models of tropospheric climate or chemistry to account for their effects. It is well known that clouds form when the vapor pressure of water exceeds the vapor pressure that would be saturated with respect to liquid water or ice. Within any

particular air mass, fluctuations in temperature and/or water vapor concentration can lead to areas where condensation (clouds) can occur even though the concentration of water averaged over the air mass may not be saturated at the mean air mass temperature.

In large-scale numerical models of the atmosphere, chemical or meteorological properties can only be explicitly resolved over relatively large air masses, typically several 10's to 100's of kilometers horizontally and ~1000 m vertically. It is not unusual to observe fluctuations in both temperature and moisture within air masses of this size due to turbulent motions, surface inhomogeneities, terrain and other factors. These perturbations induce cloud formation on a scale that cannot be resolved by larger-scale models of the atmosphere. Therefore, regional or global-scale meteorology models resort to parameterizations of cloud-induced radiative, dynamic, and chemical processes resulting from subgrid-scale clouds. In most parameterizations of cloud-scale processes, the heterogeneous (or subgrid-scale) nature of cloudiness is approximated by assuming that a fraction (f) of each grid area is occupied by clouds. This cloud fraction is used to apportion a significantly different cloud "forcing" into a "grid-averaged" forcing within grid areas that contain a mixture of clear and cloudy regions. For the results presented here, cloud cover fraction is defined as the fraction of a given horizontal plane in the atmosphere where condensed water is visibly present. This definition becomes somewhat vague when "thin" clouds are present, a condition that commonly occurs in the upper troposphere. Under these conditions, it will be difficult to explicitly quantify the fractional area of cloud coverage.

Many studies of clouds and their effects on tropospheric processes have concluded that even small cloud amounts can exert a significant influence on larger-scale processes. Under these conditions, the net effect of clouds on any physical or chemical process will be proportional to f, the fractional area of cloud coverage. Most models of tropospheric dynamics assume that the fractional area of cloud coverage is determined by the grid-averaged relative humidity. Figure 1 shows the functional dependence of cloud coverage within a particular atmospheric layer from a survey of formulations currently used by various researchers. All formulations assume a "critical relative humidity" of between 50 - 90% above which partially cloudy conditions can occur. Below

this critical humidity, all algorithms specify totally clear skies. At humidities above the critical humidity, cloud fraction increases by differing functional dependencies to 100% cloud cover at 100% humidity.

Figure 1 shows considerable differences between alternate formulations in assessing cloud coverage within current meteorology and climate models. At 80% humidity, the NCAR Community Climate Model (Williamson et al., 1987) specifies 95% cloud cover (under stable conditions), the British Meteorological Office climate model (Smith, 1990) uses 0% cloud cover, while other algorithms specify cloud coverage between these extremes.

The differences and uncertainty exhibited in Fig. 1 have motivated researchers to evaluate and improve methods for diagnosing cloud cover. Relationships between cloud cover and other meteorological factors can be quantified and evaluated using two approaches: (1) using observations of cloud cover and associated meteorology (e. g. Slingo, 1980; Sundqvist et al., 1989); and (2) inferring cloud cover from fine-resolution dynamic models capable of explicitly resolving cloud-scale dynamics (Xu and Krueger, 1991).

The primary problem with using observations to infer relationships between cloud cover and other meteorological factors is the difficulty of measuring highly-variable quantities of interest over relatively large areas. Accurate measurements capable of vertically resolving cloud coverage require high-density vertical soundings, together with satellite and relatively expensive aircraft observations. Due to the expense associated with such measurement programs, there are only limited observational datasets under a few meteorological environments from which to evaluate and improve cloud cover algorithms.

When models capable of resolving cloud-scale processes are used to ascertain cloud coverage, the accuracy and reliability of the modeling techniques are subject to an independent evaluation, which ultimately relies on observations. Sensitivities of model calculations to the model dimensionality, turbulence and microphysical parameterizations, and other factors must also be evaluated.

In this study, we compare standard meteorological observations with satellite-derived cloud coverage to ascertain the relationships between cloud coverage and other meteorological factors. We acknowledge beforehand that the standard meteorological parameters and the cloud cover measurements used in this analysis contain a considerable level of uncertainty that is difficult to quantify. However, we feel that the large size of our comparison database will allow us to ascertain the true relationships that may exist between cloud cover and other meteorological factors. With a more accurate, observation v-based method of inferring cloud cover, the global-scale influence of cloud microphysical and dynamical processes can be more accurately treated in larger-scale studies of meteorology and atmospheric chemistry.

2. Cloud cover observations

Numerous cloud cover datasets have been collected and analyzed over the past several decades. Hughes (1984) provides a summary of the characteristics of cloud climatologies available in the early 1980's. The earliest cloud climatologies were compiled solely from surface-derived observations, and were often aggregated in time at various latitudes and time of day. Cloud observations in these early archives were often composed of once-per-day observations averaged over relatively long time frames into seasonal or monthly data at a resolution of 5 - 10° latitude or longitude. Virtually all of the cloud cover datasets reviewed by Hughes (1984) were designed for use in textbooks or climate studies requiring relatively coarse temporal and spatial resolutions.

For short-term, regional-scale meteorological and chemical studies, instantaneous distributions of cloud conditions are required throughout a simulation period, updated as frequently as the underlying meteorology is changing. These models cannot readily use cloud cover estimates that are temporally averaged over large areas encompassing numerous meteorological environments. These models must use cloud coverage estimates based on shorter-term observations.

The United States Air Force Environmental Technical Applications Center has been receiving and storing Air Force Global Weather Central (AFGWC) cloud data since January 1971. From 1971 to 1983, the AFGWC used an operational real-time three-dimensional analysis of cloud

cover referred to as 3DNEPH (Fye, 1978). The 3DNEPH is a global analysis of cloud cover that uses surface-based and aircraft reports, together with visual and infrared satellite imagery to produce 3-D cloud cover information on a routine basis. During periods when satellite or surface data are lacking, clouds are inferred from rawinsonde temperatures and dew points. The data are grided onto a polar-stereographic global grid with 15 vertical layers between the surface and ~16 km above the surface. Horizontally, the grid size varies from ~25 km near the equator to ~60 km at the poles. The 3DNEPH stores cloud cover information every three hours.

Any cloud cover database will contain a level of uncertainty that is difficult to explicitly evaluate. The 3DNEPH assimilates virtually all routinely-available cloud observations into the cloud archive, making an independent evaluation impossible. Numerous unevaluated algorithms are used to consolidate surface-based observations together with visible and infrared satellite imagery. Hughes and Henderson-Sellers (1985) performed an analysis of a later version of the Air Force cloud archive (RTNEPH) for 1979, and although numerous areas of obvious but minor errors were discovered, they found that the RTNEPH observations were generally reliable and in good agreement with known features of tropospheric meteorology. Problems were found when satellite data were gathered over highly variable backgrounds or backgrounds with snow or sea ice. Also, periods of missing data are not uncommon in the data, although they are identified.

In this study, we use five noon-time spring periods analyzed over the northeast U. S. by the 3DNEPH. At noon, we expect the maximum utilization of aircraft and surface reports together with visual and infrared satellite imagery by the 3DNEPH analysis. Fig. 2 shows the cloud coverage within ~$(320\ km)^2$ areas (box shown in Fig. 2) in the layer 800 - 730 mb at local noon, 23 April 1981. The $(320\ km)^2$ averaging area corresponds to the finest "resolution" of the corresponding meteorology observations used in this analysis. During this five-day period, a relatively intense midlatitude cyclone developed and traversed the domain shown in Fig. 2. At the time of Fig. 2, the cyclone was situated near the center of the domain, and the cloud cover shows a warm frontal region over the Great Lakes, and a cold front extending from Pennsylvania to Texas. This period and domain were chosen for analysis since there are a wide variety of meteorological

conditions present from which we can determine methods to evaluate cloud coverage that may be generally applicable.

3. Standard meteorology observations

Temperature, moisture and dynamical data used in this analysis are taken from observations and spatially and temporally interpolated onto an (80 km)^2 Lambert-conformal grid using a hydrostatic mesoscale meteorology model. Observations are derived from the National Meteorological Center global meteorological analysis and further enhanced using 3-hourly surface observations and 12-hourly vertical rawinsonde measurements. Vertically, these meteorological data encompass the surface and 100 mb pressure surface (~16 km), and horizontally they span the contiguous United States. The vertical grid size of the meteorology data is ~80 m near the surface, and on the order of a kilometer or more aloft. These observations are provided as initial and boundary conditions to the NCAR mesoscale meteorological model (MM4 - Anthes and Warner, 1978). During model execution, observations are incorporated into the model calculations in regions near observation locations. Differences between observed and calculated temperatures, humidities and wind speeds are continuously minimized through the use of additional tendency terms in the momentum, moisture, and thermodynamic equations which "nudge" the calculation towards the observations. The mesoscale meteorological modeling system is not used to "predict" or "forecast" meteorology for this study. Rather, the model provides a method to enhance the spatial and temporal resolution of observed meteorology by interpolating the observations in a dynamically and physically reasonably manner. Thus, model calculations agree closely with observations when and where observations are available, and when no observations are available, the meteorological data are dynamically consistent. Meteorology interpolated and analyzed from observations in this manner provides data of superior temporal and spatial resolution relative to "raw", point observations. Since virtually all available measurements are used to "nudge" the model calculations, the temperatures, moistures, and dynamic variables resulting from this analysis agree with the measurements to within the instrument uncertainty. The uncertainty in our estimates of the meteorological state of the atmosphere in areas or times where no observations are available

is of course unknown. Stauffer and Seaman (1990) provide an analysis of the effects of observation assimilation on the quality of grided observational datasets.

Any method of extrapolating "point" measurements to larger averaging areas will introduce an uncertainty into the area-averaged "observations". With current observations, it is virtually impossible to quantify the magnitude of this "scaling-up" uncertainty. For a particular radiosonde launch, if a balloon-borne probe rises through a cloudy region of a layer of the atmosphere containing a mixture of clear and cloudy areas, it will report 100% humidity for that layer when the mean relative humidity in the layer would be well below 100%. How often these conditions occur, and just how "noisy" the temperature and water vapor fields are within areas the size of larger-scale model grid areas is a highly variable and uncertain quantity. Measurement programs to quantify these uncertainties would require high time and space resolution vertical soundings of the atmosphere under a wide variety of meteorological conditions. Until such measurements are made, there will be significant and difficult to quantify uncertainties in "measurements" of any meteorological quantity averaged over areas larger than the "footprint" area within which a measurement device operates.

Fig. 3 shows the relative humidity in the 800 - 730 mb layer interpolated from observations using the mesoscale meteorology model described above. The temperature and moisture calculations are aggregated into overlapping $(320\ km)^2$ areas, representing a 4 x 4 average of the 80 km grid used by the MM4. The domain shown in Figs. 2 - 3 represents approximately one-half of the domain simulated by the mesoscale meteorological analysis.

In Figs. 2-3, we have mapped both the cloud cover and humidity data onto the identical 320 x 320 km grid by area-averaging the "raw" temperature, moisture or cloud cover data. Vertically, the cloud cover and mesoscale interpolation model grids are slightly different, and the cloud cover grid was transposed onto the meteorology model pressure-based coordinate using a cloud volume conserving mapping. As a result, a total of 5600 data points at 15 tropospheric levels are available for comparison during the five noon-time periods studied.

4. Cloud cover under stable conditions

We expect cloud coverage to be influenced by the presence of buoyancy-induced convection that is not resolved by the coarse resolution of the meteorological observations used in this analysis. For the first portion of this analysis, we consider only areas where cumulus convection cannot occur. Local stability ($\partial T/\partial z$) at any point in a sounding is not a sufficient indicator of the presence of convective activity, since convection can often penetrate into atmospheric layers that are absolutely stable with respect to vertical perturbations (Stull, 1991). In order to define areas o layers where buoyancy-induced convection can occur, we provide a 1 m s^{-1} "push" to air with a slightly higher temperature and moisture content from each point on a vertical sounding. In a conditionally unstable environment, the "pushed" parcel will accelerate upwards. Ignoring frictional forces and pressure perturbations, the parcel velocity at levels above the layer where it is perturbed can be obtained by integrating the vertical equation of motion for a parcel rising under the influence of buoyancy accelerations:

$$\frac{dw}{dz} = \frac{g}{w}\left[\frac{T_{vp} - T_{ve}}{T_{ve}} - q_l\right] \qquad (1)$$

where w is the parcel vertical velocity, T_{vp} is the virtual temperature of the rising parcel, T_{ve} is the virtual temperature of the surrounding environment through which the parcel rises, and g is the gravitational acceleration. The condensed water content of the parcel (q_l) is the total water content (assumed to remain constant) of the parcel minus the saturated vapor mixing ratio at any level above the lifting condensation level. For this study, we define a given layer to have a potential for convective clouds if parcels are capable of rising to that layer from any layer below under the influence of buoyant forces. These areas have been neglected in the following analysis in an attempt to ascertain cloud cover under stable conditions only. We found between 1000 and 5000 stable grid areas at each of the 15 tropospheric levels during the five noontime periods considered.

a. Cloud coverage and relative humidity

The most commonly used indicator of cloud coverage is the mean relative humidity of an air mass. Others (Slingo, 1987) allow the local potential temperature lapse rate and vertical velocity to influence cloudiness. Here we hypothesize that vertical shear of the horizontal wind may also affect cloud cover. In order to evaluate whether any of these parameters are correlated with cloud coverage, we calculate the correlation coefficient for the best-fitting linear regression between cloud cover and each of these meteorological factors. While we do not expect that any of these parameters will be linearly related to cloud amount, we use this correlation analysis only as a means to initially identify how strongly each of these factors correlates with cloudiness.

Fig. 4 shows the vertical distribution of the correlation coefficient for the best-fit linear relationship between cloud cover and humidity, temperature lapse rate, wind shear, and vertical velocity. Correlation coefficients with magnitudes greater than 0.8 are considered "excellent" according to standard statistical texts, while correlations between 0.6 - 0.8 are considered "good", and correlations between 0.4 - 0.6 are only "moderate". Correlation coefficients less than 0.4 indicate poor or no relationship between parameters. This figure shows that cloud cover is most strongly correlated (positively) with relative humidity over most tropospheric layers, followed by vertical velocity, which shows moderate to good positive correlations at most tropospheric levels. There is also evidence for a weaker negative correlation between cloud cover and both wind shear and potential temperature lapse rate.

In the upper troposphere, we find almost no correlation between cloud cover and other meteorological variables. This results from two factors: (1) cloud amount and relative humidity are relatively low in this layer (~10-20% cover at 10-40% humidity); and (2) measurement uncertainty is most likely significantly greater than the mean humidities and cloud cover. It is well known that water vapor concentrations are notoriously difficult to measure at heights above the 300 mb pressure surface, and often the standard radiosonde humidities or dew points are not even reported at these heights. In addition, the highest "layers" in this analysis dataset are actually averaged over 3 - 4 km depths of the atmosphere, and therefore the "cloud area fraction" defined

above actually becomes more like a "cloud volume fraction". Both relative humidity and cloud fraction used in this analysis for the layers above the 300 mb pressure surface are highly uncertain, and any trends reported here must be interpreted with caution until better measurements are available.

In agreement with previous assumptions of factors that affect cloud coverage, Fig. 4 suggests that cloud cover is most strongly correlated with relative humidity. Using the observations shown in Fig. 2-3, we now further investigate the relationship between cloud cover and relative humidity. Data shown in these two figures together with observations from 4 additional days comprise several thousand (320 km)^2 areas where we have concurrent observations of both cloud cover and relative humidity. Fig. 5 shows the 3DNEPH cloud cover in the layer between 800-730 mb plotted as a function of the interpolated relative humidity observations at over 2300 areas where there was no potential for convection.

A high degree of scatter is immediately evident in this comparison. The correlation coefficient for the best linear relationship between cloud cover and relative humidity at this level is a relatively poor 0.64. This considerable scatter can be explained through two hypotheses: (1) cloud amount is not strongly related to relative humidity alone; and/or (2), our ability to measure both cloud amount and relative humidity over large areas is very poor. While it is difficult to explicitly evaluate the uncertainties in the meteorological parameters presented in this study without carrying out an exhaustive field measurement program, these uncertainties are most likely very large, and as a first approximation probably approach the ranges of the scatter shown in Fig. 5, i. e. 20-30% uncertainty in cloud cover, and a similar range for uncertainty in relative humidity. However, this high uncertainty does not imply that existing measurements cannot be used to assess relationships between cloud cover and related meteorological factors. If the sample size for this study is large, and covers a wide range of meteorological environments, then trends in cloud cover may be discernible, and the functional dependence of cloud cover on related meteorological parameters may be at least qualitatively revealed.

Other factors must be considered when viewing scatter diagrams like Fig. 5. Some of the scatter shown in Fig. 5 is misleading since there are several hundred points with zero cloud amount at humidities below about 45% that are literally "on top" of one another. Similarly, there are 10 - 20 coincident points at the 100% humidity and 100% cloud fraction that appear as a single point on this scatter diagram, with as much significance to the viewer as individual outlying points elsewhere on the figure. In addition, factors other than relative humidity may influence cloud cover, and thus contribute to the scatter. However, a majority of this scatter is most likely attributed to the considerable uncertainty in measuring both relative humidity and cloud cover over the large areas considered in this study.

The problem with observing cloud fraction or relative humidity over large areas is analogous to an observer using a badly out-of-focus telescope to find the location of a star in the night sky. While the telescope observer might see a light fuzzy image surrounding the true location of the object in the sky, the observer could not exactly pinpoint the object's location. However, the observer could plausibly hypothesize that the true location of the point of light is somewhere near the middle of the fuzzy image revealed by the telescope. Using similar reasoning, we hypothesize that if cloud coverage is related to relative humidity, then that relationship should fall within the range of (and most likely near the middle of) the scatter shown in Fig. 5. In assessing trends in highly uncertain measurements shown in Fig. 5, we aggregate the observations into 5% relative humidity increments, and then average the cloud coverage within these restricted humidity ranges. Using this averaging technique, trends become apparent in the highly scattered and uncertain observations. The average and standard deviation of the cloud coverage within 5% relative humidity increments are shown as a curve with error bars on Fig. 5. As expected, cloud amount increases as humidity increases. At humidities between 20 - 40%, there is 10 - 20% cloud cover on average.

This process is repeated at all tropospheric levels to obtain the average cloud cover within each layer at any particular relative humidity. Fig. 6a shows the average cloud cover within (320 km)^2 stable areas as a function of the layer relative humidity and pressure. At a particular relative

humidity, cloud amounts are greatest in the 800 - 600 mb layer of the troposphere, a trend that is consistent with earlier approximations (Buriez et al., 1988; Geleyn et al., 1982). The highest cloud amounts occur under high humidities at 900 - 800 mb, but this figure shows that 10-20% cloud coverage occurs at humidities as low as 20%, in contrast to the formulations shown in Fig. 1 which all specify zero cloud cover at humidities below 50 - 80%. Standard deviations of cloud coverage within these 5% humidity increments (Fig. 6b) fall between 20 - 30% in absolute cloud cover, which in many cases is greater than the mean cloud cover.

The trends in the average cloud amount shown in Figs. 5 - 6 suggest that fractional area of cloud coverage decreases exponentially as relative humidity falls below 100%, and that there is no clear "critical relative humidity" where cloud coverage is always zero. The trends in the average cloud amount shown in Figs. 5 - 6 suggest the following approximation for cloud amount f as a function of relative humidity Rh (Rh<1):

$$f = \exp\left\{\frac{Rh-1}{1-Rh_c}\right\} \quad . \qquad (2)$$

where

$$1-Rh_c = \begin{cases} 0.2+\frac{\sigma}{3}, & \sigma < 0.75 \\ 1.8(1-\sigma), & \sigma \geq 0.75 \end{cases} \quad . \qquad (3)$$

where σ is the pressure relative to the surface pressure (P/P_s). The ($1 - Rh_c$) term in Eq. 2 - 3 is qualitatively similar to the "critical humidity" used in previous cloud cover formulations, although here it represents the relative humidity depression from 100% where cloud amount decreases to 37% (e^{-1}). Figure 7 shows the value of ($1 - Rh_c$) in Eq. (2) that yields the minimum root mean square difference between observed cloud amount and cloud amount calculated using Eq. (2). Also shown on this figure are contours of the root mean square difference between cloud amount calculated using Eq. (2) and observed cloud amount as a function of the values chosen for the ($1 - Rh_c$) parameter. Individual data points represent the value of ($1 - Rh_c$) which produces the minimum error, and the two linear segments plotted show Eq. (3), a simple formula that attempts to stay near the areas of lowest error at each tropospheric level. Using Eq. (2) to calculate cloud

cover from relative humidity [both averaged over $(320\ km)^2$ areas] produced cloud cover estimates that on average contained a root mean square difference of 7 - 25 percentage points from the 3DNEPH observations, depending on the tropospheric level considered.

b. Cloud coverage and vertical velocity

As shown in Fig. 4, vertical velocity is another parameter which influences cloud coverage almost as significantly as relative humidity. Some of the scatter about the mean shown in Figs. 5 - 6 may result from deviations in vertical velocity within a restricted relative humidity range. In order to estimate the effects of vertical velocity on cloud coverage, we further subdivide observations into 1 cm s^{-1} vertical velocity increments, and investigate relationships between vertical velocity and cloud cover. Fig. 8 shows the observed correlation between cloud cover and vertical velocity in the 800 - 730 mb layer with relative humidity restricted to 50 - 55%. While the correlation between vertical velocity and cloud cover is weak at this particular atmospheric level, there is a discernible trend in the cloud cover if observations are aggregated into 1 cm s^{-1} increments. In order to facilitate the identification of trends, we have superimposed the nearly linear trend in aggregated cloud cover observations over the scattered observations. This figure shows that some of the scatter in the 50 - 55% humidity range shown in Fig. 5 can be attributed to variations of vertical velocity. A bulk of the low cloud amounts observed at this humidity have vertical velocities <-1 cm s^{-1}, while there are very few clear skies ($f = 0$) when the vertical velocity is positive.

In order to quantify the influence of vertical velocity on cloud cover, we calculate the "critical humidity" term $(1 - Rh_c)$ in Eq. 2 that yields the lowest root mean square differences between the observed cloud cover and cloud cover calculated using Eq. 2 using observations confined to 1 cm s^{-1} vertical velocity increments. Fig. 9 shows the functional dependence of this critical humidity depression as a function of vertical velocity for the two tropospheric layers. These data show an approximately linear relationship that is reproduced at all other tropospheric levels. The fractional area of cloud coverage when the vertical velocity is close to zero is best

approximated by Eq. 3, and Fig. 10a shows the vertical variation of the slope of the best-fitting line through the data shown in Fig. 9 for all tropospheric levels. Therefore, if both relative humidity (Rh) and vertical velocity (w - cm s^{-1}) are used to estimate cloud coverage, we propose the following formulations:

$$c = \exp\left\{\frac{Rh - 1}{\max\left[(1 - Rh) + 0.1\sigma^2 w, 0.001\right]}\right\} \qquad (4)$$

Again, σ is the pressure relative to the surface pressure (P/P_s), and the ($1 - Rh_c$) term in the denominator is specified in Eq. 3. As shown in Fig. 10b, using both humidity and vertical velocity (Eqs. 3 - 4) to specify cloud cover reduces the root mean square deviations from the 3DNEPH cloud cover by less than 10 percent relative to using only relative humidity (Eq. 2 - 3). The calculations of Eq. 4 applied to one humidity range and level are also plotted as the curve identified in Fig. 8. For this particular level and relative humidity range, the parameterization produces a slight overestimate of cloud cover, although the sensitivity of the cloud cover to changes in vertical velocity are well simulated. At other relative humidity intervals and levels, Eq. 4 produces better or worse agreement with the trends revealed by these observations, and on average, the formulation suggested above produces the best overall approximation. More complicated formulations employing additional free parameters were investigated, but the additional complexity of the formulations did not significantly reduce the differences between observed and calculated cloud cover relative to the formulations described above.

5. Cloud cover under convectively unstable conditions

We now consider regions where buoyancy-induced convection can influence cloud coverage. As noted above, convectively unstable areas are defined as regions in the atmosphere where parcels that are slightly less dense than their surrounding environment can rise to after being given a minor impulse. Fig. 11 shows the average cloud cover within (320 km)^2 unstable areas as a function of the layer relative humidity and pressure. This figure is qualitatively similar to Fig. 6 showing cloud cover under stable conditions: i. e. cloud amount maximizes in the middle

troposphere. Fig. 11b shows the difference between the stable and unstable cloud covers f_{stable} - $f_{unstable}$ at the same relative humidity and pressure. Since the observations from which these figures are constructed contain a high level of scatter, some of the differences between stable and unstable cloud covers may not be statistically significant. Therefore, we perform a chi-square analysis of these differences. Relative humidity and cloud cover data pairs were aggregated into 10% cloud cover increments at each 5% humidity increment and pressure level. The unstable and stable cloud cover frequency distributions were then subjected to a chi-square confidence limits test. Differences between stable and unstable cloud cover that are significant at greater than the 95% confidence limit are denoted by heavy Xs on Fig. 11b, and differences that are significant at greater than the 90% limit are denoted by plain Xs. Differences that are not close to an "x" on Fig. 11b are usually small and may not be statistically significant.

Fig. 11 shows that under relatively humid convectively unstable conditions, we see evidence for increased cloud amounts relative to stable conditions at the same humidity in the upper troposphere. In the lower troposphere, high humidity environments where convection is possible contain lower cloud amounts relative to stable conditions at the same relative humidity, which may result from the subsidence of dry air into the lower troposphere under convectively unstable conditions. These differences seem physically reasonable. However, under unstable conditions there is a region of significantly lower cloud amounts when humidities are below 65% in the upper troposphere that cannot be easily explained. This anomalous behavior prompted a further investigation of the cloud cover and humidity data. Further analysis of the MM4 interpolation system showed that under unstable conditions, the upper troposphere is calculated to become rapidly saturated when observations are not assimilated into the model forecast equations (i. e. the MM4 is run in a "forecast" mode away from the model boundaries). The MM4 calculates humidities approaching 80 - 100% in the layer from 500 - 100 mb over the region of convective storms associated with transient cold and warm fronts. Simultaneous observations showed much smaller regions of humidities in excess of 80% between 500 - 300 mb, and above 250 mb, relative humidities never exceeded 20%. As noted previously, these upper-tropospheric relative humidities

are notoriously unreliable. However, the differences between the calculated humidities and "observed" humidities are considerable in the regions of frontal convection. For the version of the model used in this analysis, any biases introduced by the model physics into the calculation of water vapor that is partially deleted since water vapor calculations are continuously "nudged" towards the relatively dry observations. Despite this correction, there is a possibility that under convectively unstable conditions, there may be a bias in the MM4-produced moisture calculations that employ the moisture-convergence based convective parameterization. If this is the case, then the relative humidities used to construct Fig. 11 may be higher than were actually present, especially under the unstable conditions when the MM4 convective parameterization was calculating higher moistures than observed in the upper troposphere.

Thus, we see an inconsistency between the MM4 humidity calculations and the 3DNEPH cloud cover under unstable conditions. Cloud amounts typical of relatively low humidities under stable conditions are being observed at the higher humidities calculated by the MM4 in unstable areas. Since observed humidities above about 300 mb are highly uncertain, and possibly significantly lower than the MM4 calculations when it is exercised in a predictive mode, it appears that humidity calculated using MM4 under convectively unstable conditions may be overestimated. In short, there are very few clouds observed where the MM4 is calculating 80 - 100% humidities, suggesting that the humidities may be too high.

Because of these apparent discrepancies, we feel that we cannot reliably use the observation-interpolation system described above to derive relationships between cloud cover and humidity under unstable conditions. More accurate methods of correlating cloud cover and relative humidity or other meteorological factors will require more accurate methods of inferring moisture distributions over large areas, particularly within convectively unstable areas. This apparent discrepancy may also influence humidity "measurements" reported here under stable conditions in the upper troposphere since this is an integrated observation assimilation system, although these errors would be continuously minimized in areas where observations are available. However, as noted earlier, in the upper troposphere where even direct measurements of water vapor are highly

uncertain, any formulations representing relationships between cloud cover and humidity derived from those measurements are open to considerable uncertainty.

6. Discussion and Conclusions

In this study, we have compared satellite observations of fractional cloud coverage within ~(320 km)^2 areas with related meteorological observations over the northeast U. S. during a springtime midlatitude cyclone. Cloud cover observations were derived from the U. S. Air Force 3DNEPH analysis of satellite imagery, aircraft reports, and surface-based observations. Other meteorological measurements were interpolated from radiosonde observations using a hydrostatic mesoscale meteorology model. Co-located comparisons of the cloud cover with other meteorological measurements show considerable uncertainty, although we find moderate correlations between cloud cover and relative humidity and vertical velocity. An analysis of the relationship between observed cloud cover and humidity suggests that cloud cover decreases exponentially as humidity falls below 100%. Relative to other layers in the troposphere, the middle troposphere (700-500 mb) contains higher cloud amounts at lower humidities, with mean cloud amounts of ~30% near 50% humidity. At the same relative humidity, cloud cover increases with increasing vertical velocity, and cloud cover also exhibits weak negative correlations with potential temperature lapse rate and vertical shear of the horizontal wind.

The analyses described above were repeated at several different horizontal averaging resolutions. The fundamental observations were horizontally averaged from areas representing the horizontal grid size of the meteorological interpolation model (80 km) up to 8 x 8 averages (640 km) of the finest resolution observations. There were only minor quantitative fluctuations of the correlations described above, and the only parameters which changed significantly were the root mean square deviations and the correlation coefficients between formulations of cloud cover based on other meteorological factors. As the horizontal averaging area became larger, the "scatter" (e. g. see Fig. 5) became smaller as numerous grid areas with deviations became merged into a single area. Thus, the above-described methods for estimating cloud cover within a particular atmospheric layer should be applicable for all model grid sizes > 80 km.

Under conditions when buoyancy-driven vertical motions are possible, we find some discrepancies between model calculations of relative humidity and the cloud cover observations, suggesting a bias in the method of interpolating relative humidity in the upper troposphere. In particular, we see low cloud amounts that are typical of much drier conditions occurring at higher humidities under unstable conditions, which we attribute to excessive vertical transport of water vapor under convective conditions. We are thus using the 3DNEPH cloud observations as an evaluation tool. In a manner similar to Nehrkorn and Hoffman (1990), our analysis suggests that cloud coverage may be a useful tool to infer relative humidity, contrary to the underlying purpose of most cloud cover algorithms: to infer cloud coverage from other "easy to estimate" meteorological factors. For inferring upper tropospheric water vapor concentrations, perhaps satellite-derived cloud coverage is a parameter that is easier to estimate with greater accuracy than relative humidity.

Despite the high level of uncertainty present in this analysis of cloud cover, it is obvious that most parameterizations of cloud coverage used by current climate models calculate smaller cloud amounts than reported by the 3DNEPH observations, especially in middle tropospheric levels at relative humidities less than 70 - 80%. It is apparent that many cloud cover formulations shown in Fig. 1 assume that cloud cover fractions are considerably lower than the mean minus one or more standard deviations from the measurements presented in Fig. 5. The differences between current formulations and these observations is greatest at low humidities. Many of the formulations for cloud cover used by climate models are not actually based on short-term observations of cloud cover and relative humidity. Rather, these formulations along with their "critical humidities" are "tuned" within the context of their host model physics and dynamics to yield reasonable estimates of the global, long-term planetary albedo. Thus, cloud cover formulations are "backed-out" of their host model, and represent a functional form which when used in the particular climate model for which they were tuned, yield a reasonable planetary albedo. The danger of this method of assessing cloud cover is that other model uncertainties and even errors can be compensated for by an incorrect cloud cover formulation. For example, if a model

uses an optical depth for clouds that is too great, then this error can be compensated for by making the clouds smaller (i. e. a smaller cloud fractional coverage). Most cloud cover formulations appear to calculate cloud amounts that are considerably smaller than reported in the 3DNEPH archive, yet these same climate models claim to reproduce the global planetary albedo accurately. This suggests that other components of climate models may be uncertain or in need of improvement.

These results suggest that current methods of calculating cloud coverage within large-scale climate simulations or atmospheric chemical modeling studies are significantly underestimating cloud amount at most relative humidities. More importantly, current climate models probably cannot adequately estimate the potentially significant changes in cloud cover that can result from small changes in relative humidity. As is clearly shown in Fig. 1, a small change in relative humidity can result in large or small changes in cloud coverage, depending on which cloud cover algorithms are used. This analysis of the 3DNEPH cloud archive shows an exponentially decreasing cloud cover as relative humidity decreases, and no clear "critical relative humidity" below which there are no clouds. More importantly, according to the trends revealed by this analysis, cloud amount probably changes as relative humidity changes at *any* relative humidity, unlike current formulations, which only allow cloud cover to change when relative humidity is greater than 60 - 90%.

Acknowledgments. The author is grateful to the organizations that are supporting portions of the research presented here: the U. S. National Science Foundation under grant ATM-9014933; the U. S. Department of Energy under grant DE-FG02-92ER61364; and the U. S. Air Force Office of Scientific Research under grant F49620-92-J-0018.

REFERENCES

Anthes, R. A. and T. T. Warner, 1978: Development of hydrodynamic models suitable for air pollution and other mesometeorological studies. *Mon. Wea. Rev.*, **106,** 1045-1078.

Arakawa, A. and W. H. Schubert, 1974: Interaction of a cumulus ensemble with the large-scale environment, part 1. *J. Atmos. Sci.*, **31,** 674-701.

Buriez, J.-C., B. Bonnel, Y. Fouquart, J.-F. Geleyn, and J.-J. Morcrette, 1988: Comparison of model-generated and satellite-derived cloud cover and radiation budget. *J. Geophys. Res.* **93,** 3705-3719.

Fye, F. K., 1978: The AFGWC automated cloud atlas model. AFGWC Technical Memorandum 78-002. HQ Air Force Global Weather Central, Offutt AFB, Nebraska 68113, 58 pp.

Geleyn, J.-F., A. Hense and H.-J. Preuss, 1982: A comparison of model-generated radiation fields with satellite measurements. *Beitr. Phys. Atmosph.*, 55, 253-286.

Hughes, N. A., 1984: Global cloud climatologies: a historical review. *J. Appl. Clim. and Meteor.*, **23,** 724-751.

Hughes, N. A. and A. Henderson-Sellers, 1985: Global 3D-nephanalysis of total cloud amount: climatology for 1979. *J. Appl. Clim. and Meteor.*, **24,** 669-686.

Nehrkorn, T. and R. N. Hoffman, 1990: Inferring relative humidity profiles from 3DNEPH cloud data. J. Appl. Meteor., 29, 1330-1343.

Ramanathan, V., E. J. Pitcher, R. C. Malone and M. L. Blackmon, 1983: The response of a spectral general circulation model to refinements in radiative processes. *J. Atmos.Sci.*, **40,** 605-630.

Slingo, J. M., 1980: A cloud parameterization scheme derived from GATE data for use with a numerical model. *Quart. J. Roy. Met. Soc.*, **106,** 747-770.

Slingo, J. M., 1987: The development and verification of a cloud prediction scheme for the ECMWF model. *Quart. J. Roy. Met. Soc.*, **113,** 899-927.

Smith, R. B. N. 1990: A scheme for predicting layer clouds and their water content in a general circulation model. *Quart. J. Roy. Met. Soc.*, **116,** 435-460.

Stauffer, D. R. and N. L. Seaman, 1990: Use of four-dimensional data assimilation in a limited-area mesoscale model. Part 1: experiments with synoptic-scale data. *Mon. Wea. Rev.*, **118,** 1250-1277.

Stull, R. B., 1991: Static stability-an update. *Bull. Am. Met. Soc.*, **72,** 1521-1529.

Sundqvist, H., E. Berge, and J. E. Kristjánsson, 1989: Condensation and cloud parameterizations studies with a mesoscale numerical weather prediction model. *Mon. Wea. Rev.*, **117,** 1641-1657.

Walcek, C. J., W. R. Stockwell, and J. S. Chang, 1990: Theoretical estimates of the dynamic, radiative and chemical effects of clouds on tropospheric trace gases. *Atmos. Res.*, **25,** 53-69.

Williamson, D. L., J. T. Kiehl, V. Ramanathan, R. E. Dickinson, and J. J. Hack, 1987: Description of the NCAR Community Climate Model (CCM1). NCAR Technical Note NCAR/TN-285+STR, National Center for Atmospheric Research, Boulder, CO 80307.

Xu, K-M and S. K. Krueger, 1991: Evaluation of cloudiness parameterizations using a cumulus ensemble model. *Mon. Wea. Rev.*, **119,** 342-367.

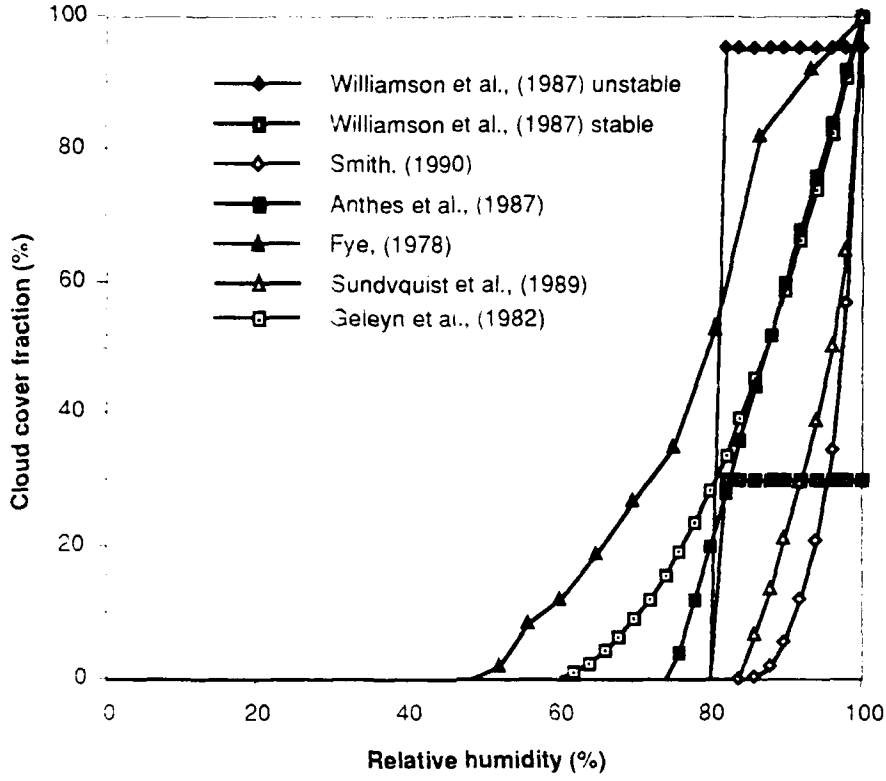

FIG. 1. Fractional cloud coverage as a function of relative humidity at 800 mb according to various formulations used by meso- and global-scale atmospheric models.

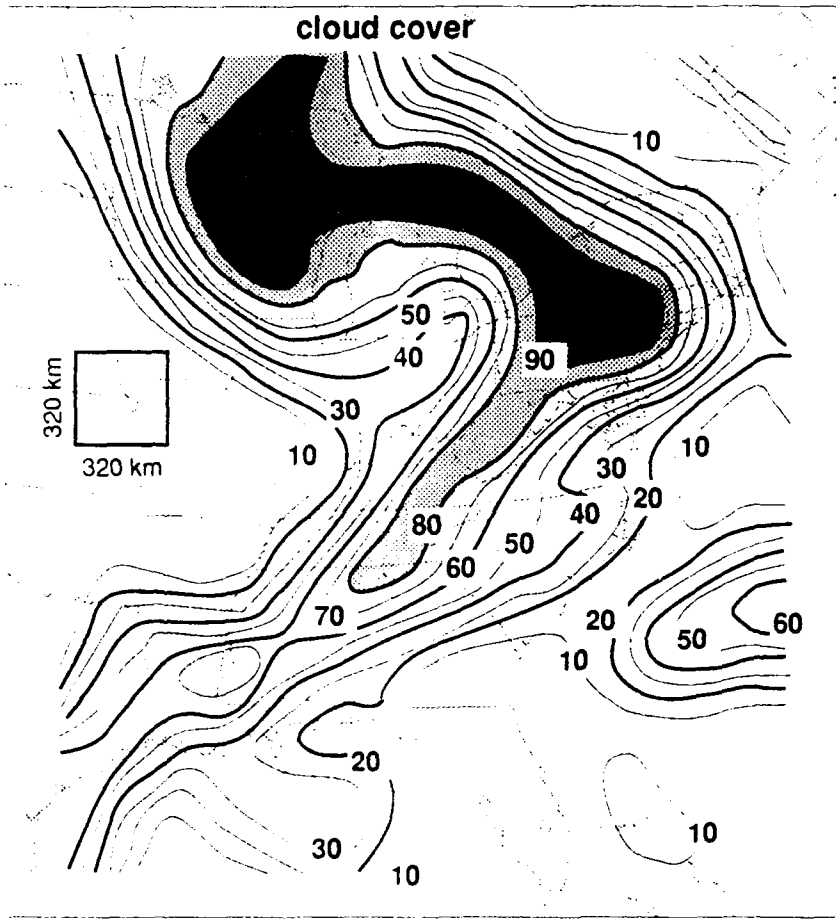

FIG. 2. Cloud cover averaged over (320 km)^2 areas (box shows a sample area) in the layer 800-730 mb at 18 UT, 23 April 1981 according to the U. S. Air Force 3DNEPH compilation of surface reports, aircraft observations, and satellite-derived data.

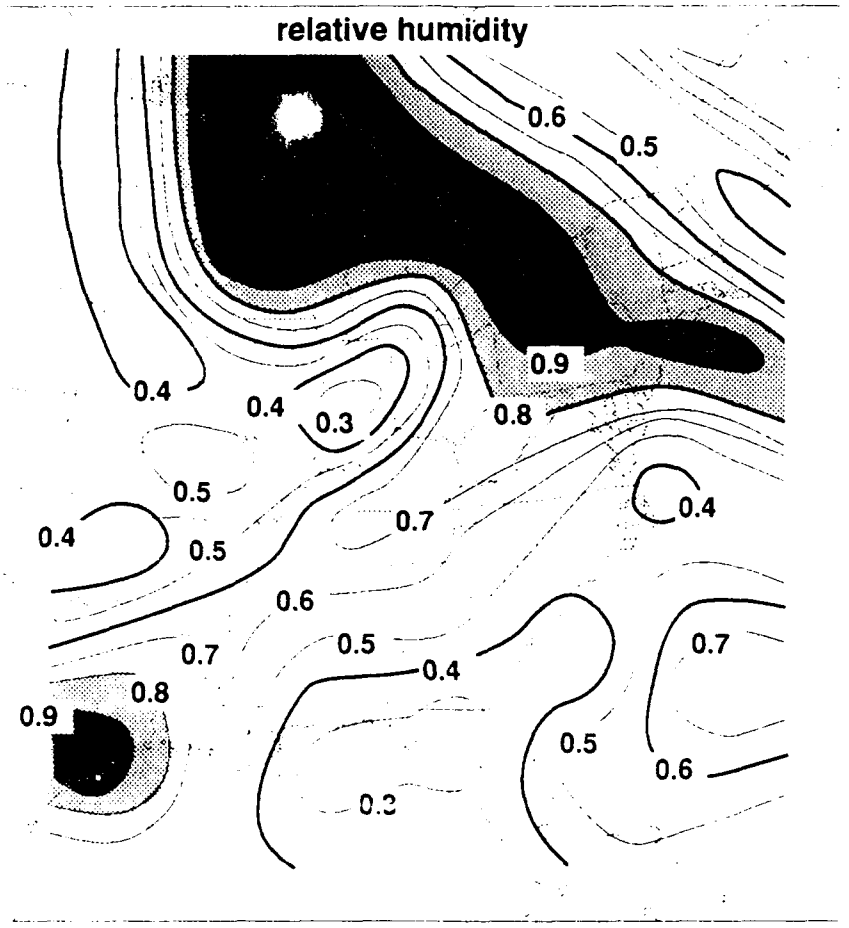

FIG. 3. Relative humidity averaged over (320 km)^2 areas in the layer 800-730 mb at 18 UT, 23 April 1981 interpolated from grided NMC observations in time and space using a hydrostatic mesoscale meteorology model.

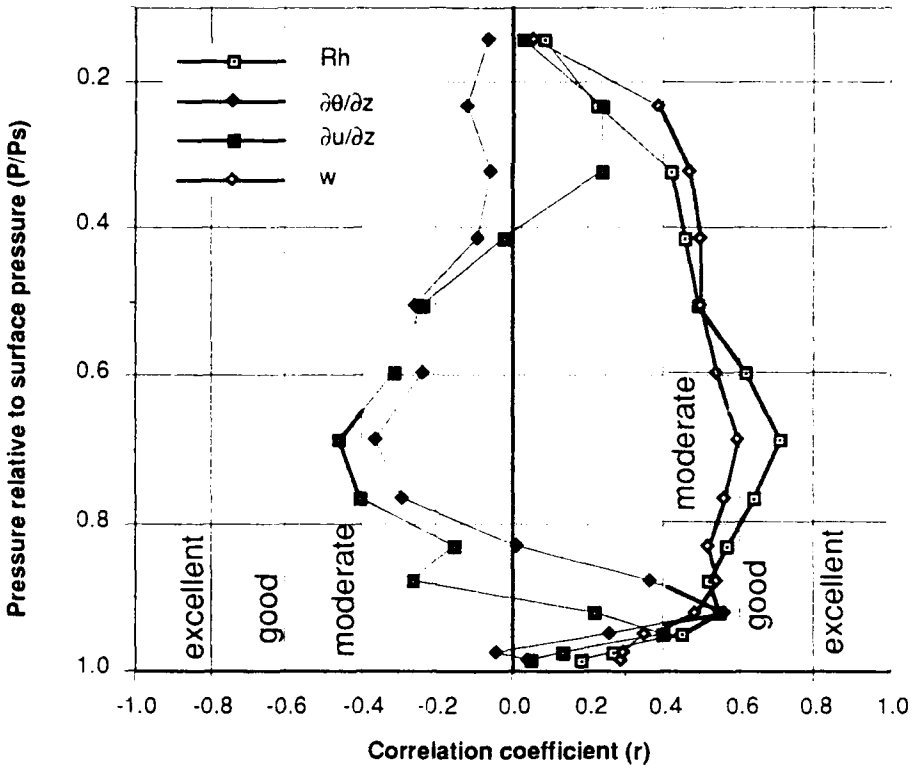

FIG. 4. Correlation coefficient at various atmospheric levels for the best-fit linear relationship between cloud cover and relative humidity, potential temperature lapse rate, wind shear, and (320 km)^2 averaged vertical velocity.

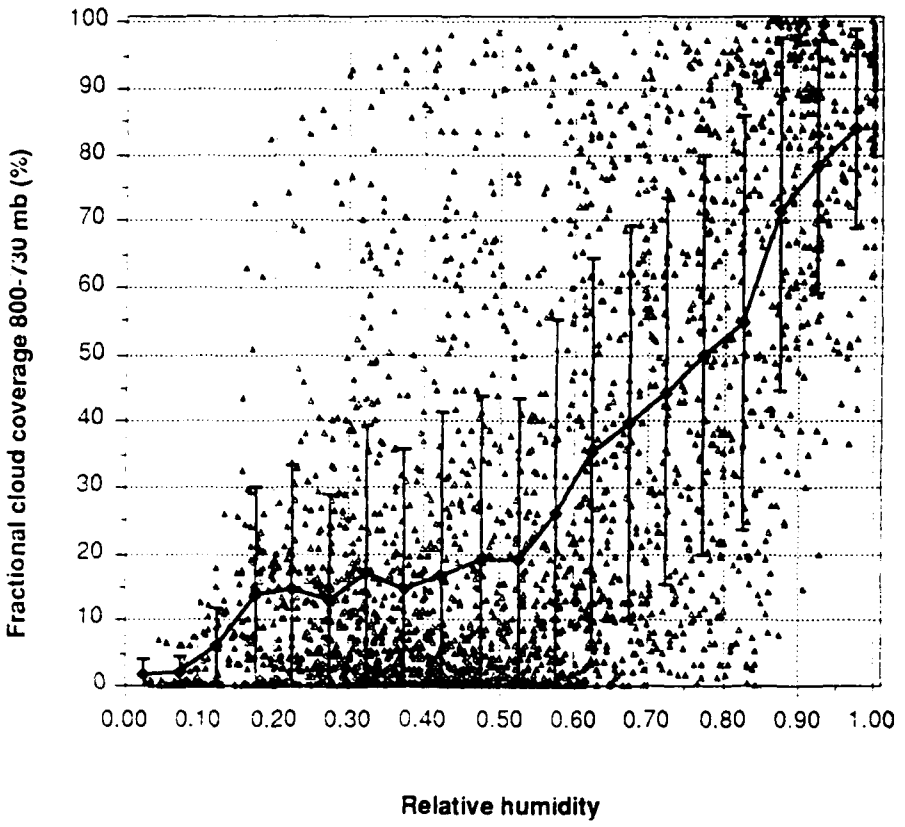

FIG. 5. Fractional cloud coverage as a function of relative humidity at 800-730 mb. Each point represents one (320 km)^2 area in the domain shown in Fig. 3 during 20-24 April 1981. Only grid areas where no buoyancy-driven convection can occur are considered. Lines show the mean and standard deviation of cloud cover within 5% increments of relative humidity.

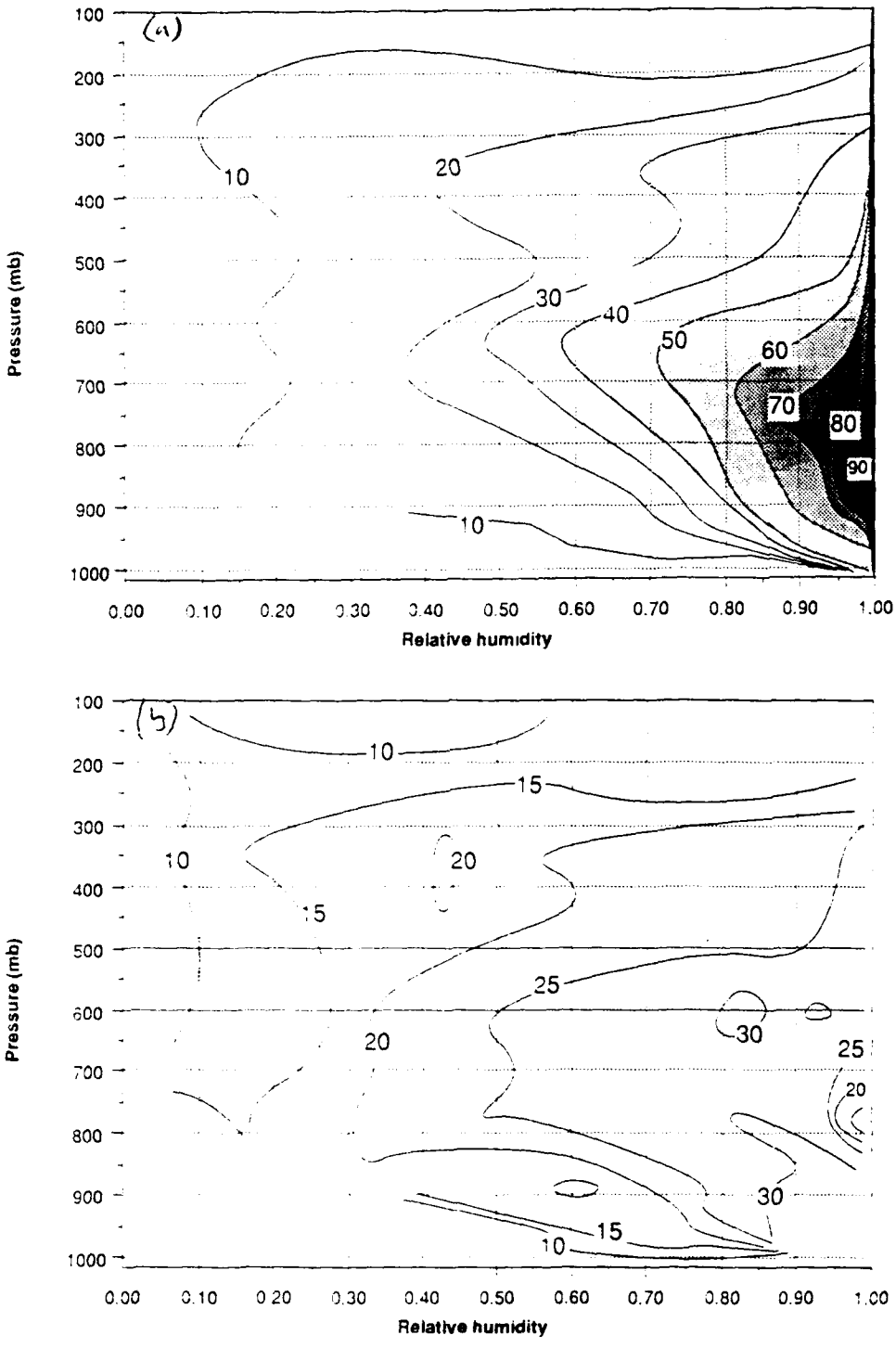

FIG. 6. (a) Fractional cloud coverage and (b) standard deviation of fractional cloud coverage as a function of relative humidity and pressure during 20 - 24 April 1981 over the northeast U. S. shown in Fig. 3. Only areas where no convection occurs are used to construct this figure.

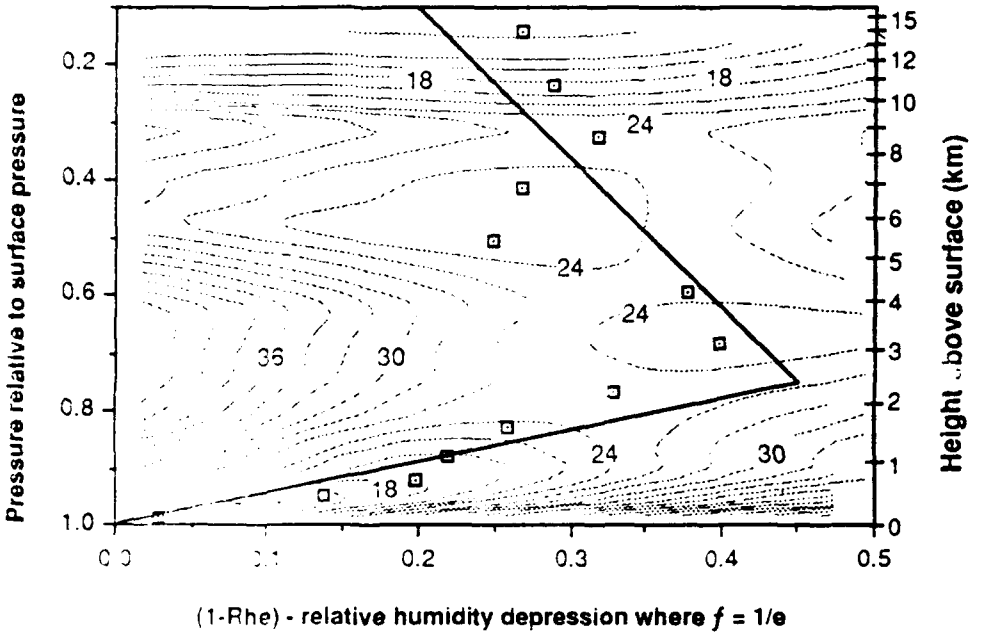

FIG. 7. Contours of the root mean square error (% cloud cover) in calculating cloud amount from relative humidity using Eq. (2) as a function of values for the critical humidity depression ($1-Rh_c$) and pressure level in the atmosphere. Points represent the values for ($1-Rh_c$) that yield the minimum difference between observed and calculated cloud faction. Solid curve shows Eq. (3), the suggested vertical variation of ($1-Rh_c$).

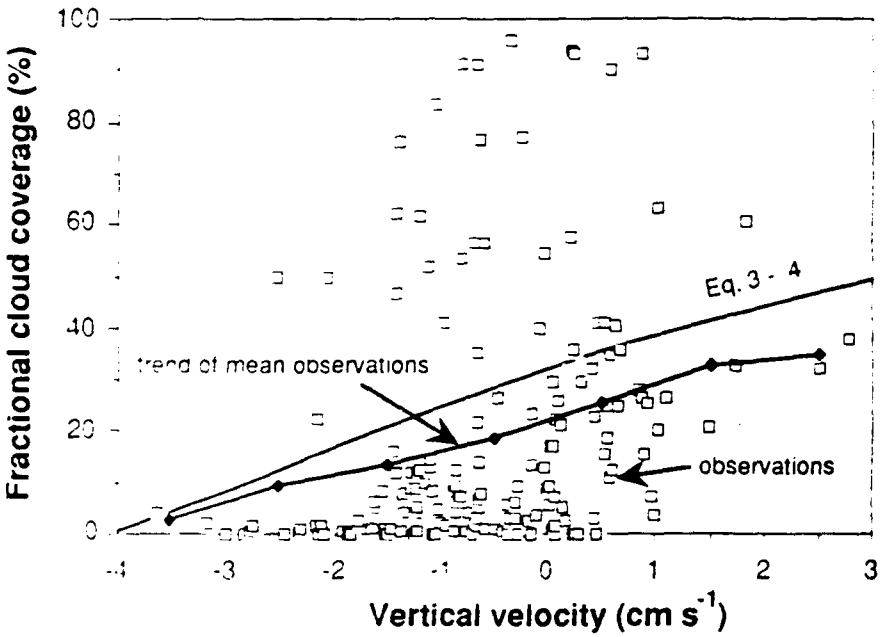

FIG. 8. Fractional cloud coverage as a function of vertical velocity at 800-730 mb. relative humidity between 50 - 55 %. Each point represents one (320 km)^2 area in the domain shown in Fig. 3 during 20-24 April 1981. Only grid areas where no buoyancy-driven convection can occur are considered. Line identified as "trend" shows the mean cloud cover within 1 cm s^{-1} vertical velocity increments. Line identified as "Eq. 3-4" shows cloud amount calculated using Eq. 3 - 4.

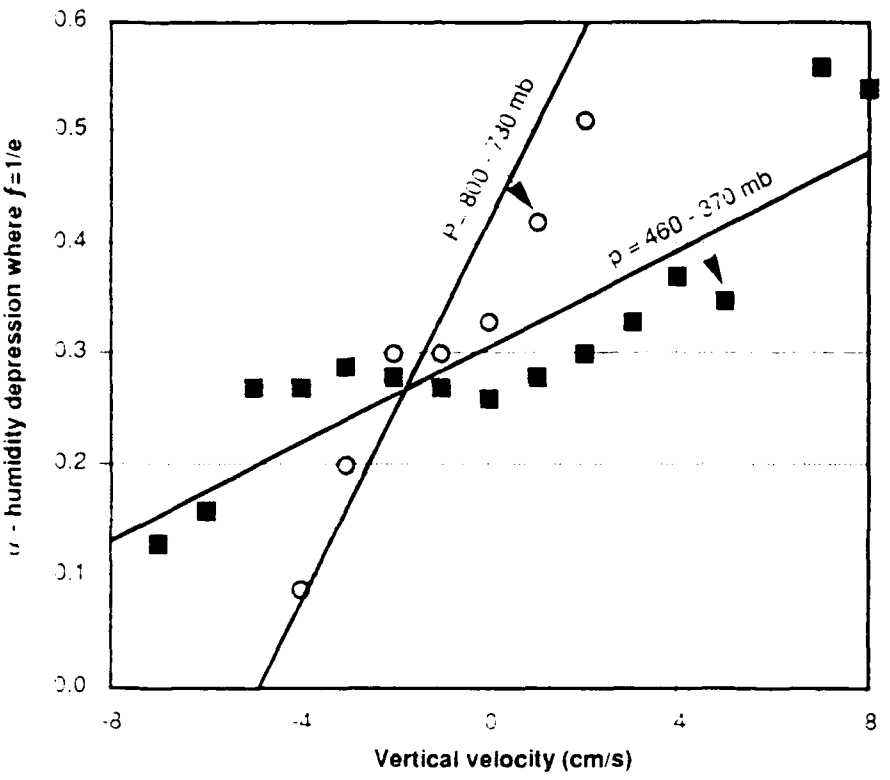

FIG. 9. Critical relative humidity depression that yields minimum root mean square difference between calculated and observed cloud cover as a function of vertical velocity at the 800 - 730 mb layer.

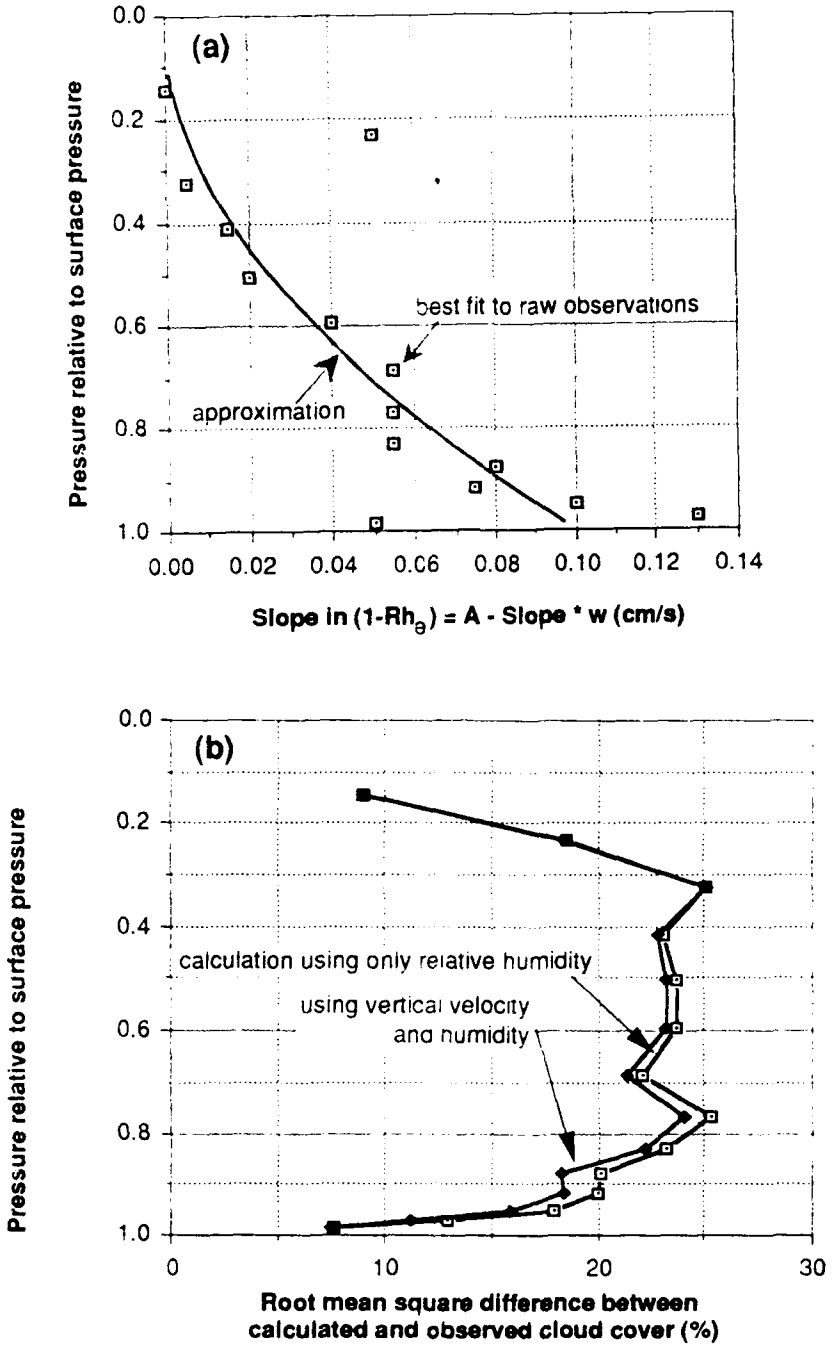

FIG. 10. (a) Vertical variation of the sensitivity of critical relative humidity depression to vertical velocity (Rh change per cm s^{-1} - slope of best fitting line shown in Fig. 9). Data points plotted are the values in Eqs. 4 which yield the minimum RMS difference between 3DNEPH and cloud cover calculated from relative humidity and vertical velocity. (b) Root mean square differences between cloud cover calculated using Eqs. 2 - 4 and observed cloud cover during 20 - 25 April 1981.

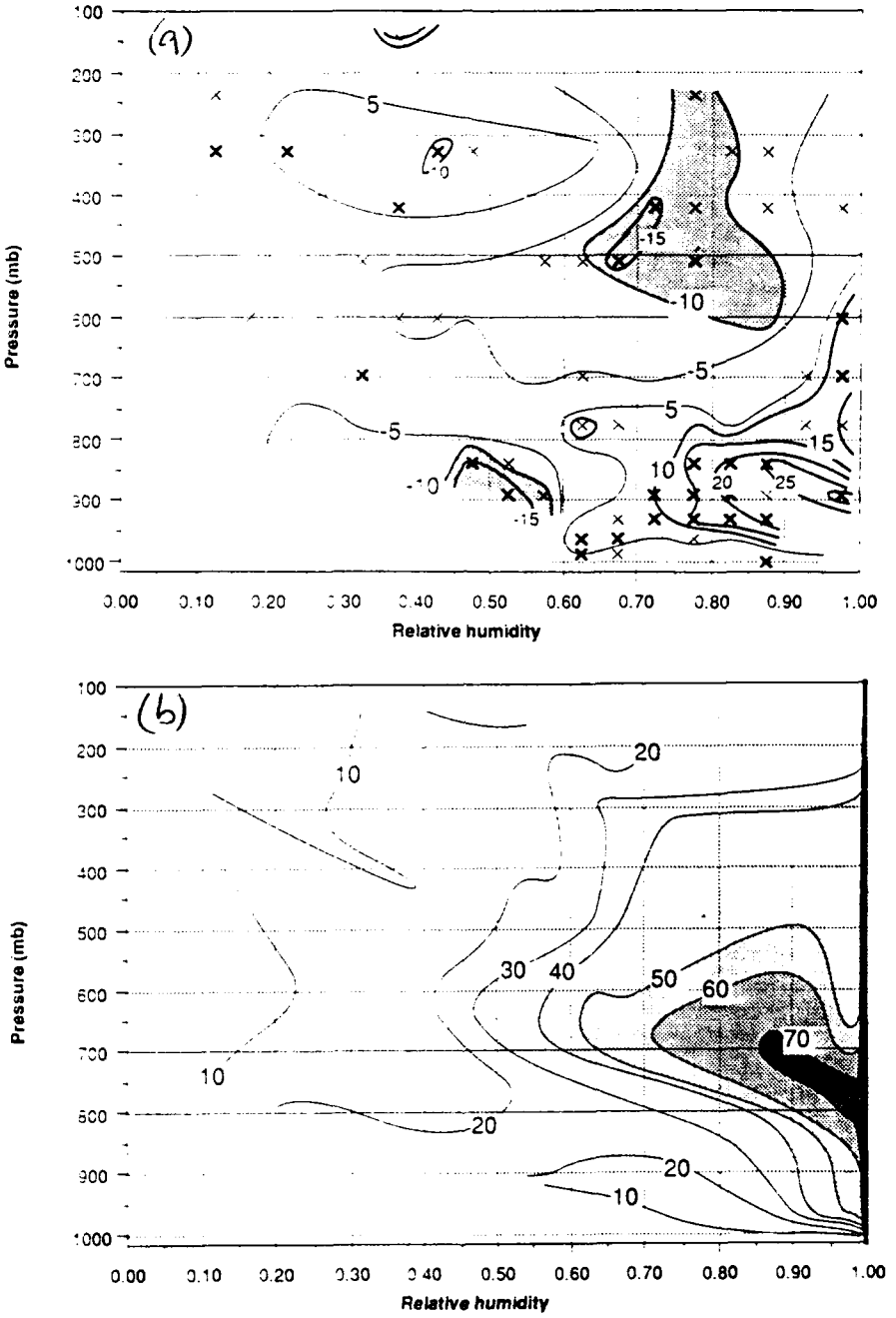

FIG. 11. (a) Fractional cloud coverage as a function of relative humidity and pressure during 20 - 24 April 1981 over the northeast U. S. (domain shown in Fig. 3). Only areas where buoyancy-driven convection can occur are considered in this figure. (b) Difference between stable and unstable cloud cover (f_{stable} - $f_{unstable}$, Fig. 6a - Fig. 11a) as a function of relative humidity and pressure. Heavy x's denote differences that are significant with greater than 95% confidence, lighter x's denote differences that are significant above a 90% confidence threshold. All other areas contain differences that are significant at less than 90% confidence. Shaded areas in Fig. 11b show areas where cloud cover is greater under convectively unstable conditions relative to stable conditions at the same pressure and relative humidity.